825. Evaluation of the natural draught cooling tower shell using linearly and non-linearly numerical analysis

Sam-Young Noh[1], Sang-Yun Lee[2]
Department of Architectural Eng., Hanyang University, Ansan, Korea
E-mail: [1]*noh@hanyang.ac.kr*, [2]*yongsha@naver.com*

(Received 30 July 2012; accepted 4 September 2012)

Abstract. The shell shape of the natural cooling tower determines the sensitivity of the whole structure against wind excitation. This study analyses influence of the tower shell geometric parameters on the structural behavior, evaluated by linearly and nonlinearly numerical analyses. The goal of the study is to give an informative statement for the form-finding process of the cooling tower shell in the engineering practice. The generated 32 towers from an existing cooling tower are linearly analyzed base on the natural frequency. Further three representative models were selected, they were analyzed based on the buckling factor and the reinforced amount required according to a design guideline. The hyperbolic shell with overall radii as small as possible yielded not only a higher first natural frequency, thus less wind-insensitivity, but also a safer buckling behavior and a economical design due to less requirement of concrete and reinforcement. This advantageous structural behavior could be consistently verified in the nonlinear analysis, evaluated by load-deformation curves and damage indices based on the natural frequencies and modal contribution factors.

Keywords: natural draught cooling tower, hyperbolic shell geometry, natural frequency analysis, nonlinear FE-analysis, global damage indicator.

1. Introduction

In the design procedure of the cooling tower the form-finding of the shell is the most important process, because the shape of the shell determines the sensitivity of dynamic behavior of the whole tower against wind excitation. In engineering practice, geometric parameters of the shell are generally determined based on natural frequency analysis. The goal in the design is the optimization of the required reinforcement steel while satisfying target safety factors.

The previous works by Busch et al. [1] and Harte et al. [2], which reported influences of the throat height and the angle of the base lintel for the shape optimization of the cooling tower shell, give excellent motivation for further research. In the study the geometric parameters were analyzed more in detail. 32 cooling tower shell geometries were selected through variation of the geometric parameters of an existing cooling tower shell. They were evaluated based on the first natural frequency. From the result three representative cooling towers are selected for the analysis of the structural behavior by means of linear and nonlinear FE-method.

2. Cooling tower shell geometry

The cooling tower shell generally consists of one or two rotationally symmetrical hyperbolic shells. The overall geometric parameters of the shell hyperbolas like total height, column height and minimum shell diameter are determined based on thermo-dynamical requirements – the thermodynamic parameters. Three parameters are left for optimization of the shell hyperbolas with respect to structural specifications - angle of the base lintel, height of the throat and diameter of the top lintel (Table 1). They determine static and dynamic characteristics of the shell structure. The established generator equation for an axisymmetric hyperbolic shell is given over the height of z, as in equation (1). Herein, Δr = distance between hyperbolic axis and rotational axis, A = minimum distance between hyperbolic axis and rotational axis and

B = curvature parameter. They can be determined using the boundary conditions: $r\ (z = 0) = r_t$, $r\ (z = h_u) = r_u$ and $r'\ (z = h_u) = \varphi_u$:

$$r = \Delta r + A\sqrt{1 + \left(\frac{z}{B}\right)^2} \ . \tag{1}$$

The structural parameters in Table 1 are geometrically limited as given in Table 2. They can be obtained by the consideration of the boundary conditions of the hyperbolic shape and the geometric constants A and B.

Table 1. Geometric parameters of hyperbolic cooling tower shell

Thermodynamic parameters	▪ Total height h ▪ Height of column h_c ▪ Radius of base lintel r_u ▪ Radius of throat r_t	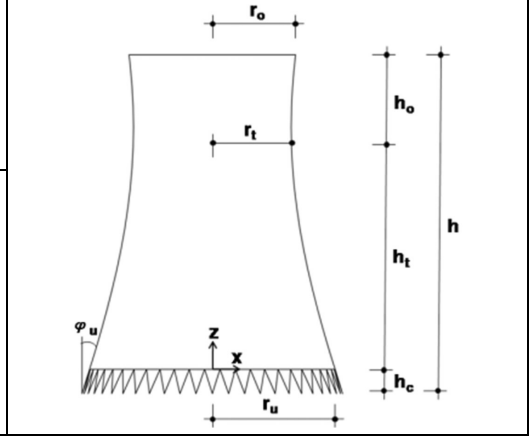
Structural parameters	▪ Angle of base lintel φ_u ▪ Height of throat h_t ▪ Radius of top lintel r_o	

Table 2. Limits of the structural parameters

Height of throat h_t	$h_c + \frac{r_u - r_t}{\tan\phi_u} < h_t < h$
Angle of base lintel φ_u	$\arctan\left(\frac{r_u - r_t}{h_u}\right) < \phi_u < \arctan\left(2\frac{r_u - r_t}{h_u}\right)$
Radius of top lintel r_o	$r_t \le r_o \le r_t + \frac{1}{2}\left(h_o^2 \cdot \frac{A_u}{B_u^2}\right)$

3. Parameter study based on first natural frequency

3. 1 Selection of cooling tower shell geometries

For simplifying the problem, a cooling tower consisting of one hyperbolic shell was considered as a prototype tower in this study. This cooling tower shell is characterized by the thermodynamic parameters; height h = 150.00 m, radius r_t = 35.08 m, radius of base lintel r_u = 54.65 m, supported by 50 V-columns with height h_c = 10.80 m. The structural parameters of the prototype are a top lintel radius r_o = 37.08 m, the height of throat h_t = 118.00m and the angle of base lintel φ_u = 17.72°. An overview of the cooling tower is shown in Fig. 1. The limits of the available structural parameters are given in Table 3.

In order to investigate the influence of structural parameters on the structural behavior, the parameters of the original tower have been varied and studied with respect to their structural

characteristics. The height of the throat was changed with an interval of 5 m and the angle of the base lintel with an interval of 1°. Thus considering the valid range of possible structural parameters, totally 32 evaluation models were selected with h_t = 128 m, 123 m, 118 m, 113 m, 108 m and φ_u = 15°, 16°, 17°, 17.72°, 18°, 19°, 20°.

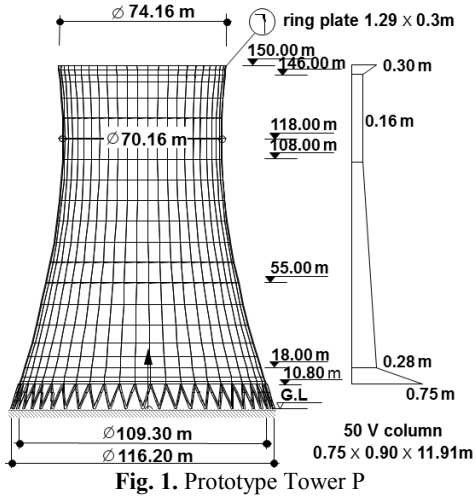

Fig. 1. Prototype Tower P

Table 3. Structural properties and generator parameters

Material and other properties			
Shell	HD500	E_c	25 MN/m^2
Column			35 MN/m^2
Single footing	E / D / B		4.0 m/5.0 m/1.5 m
	$C_x = C_y = C_z$		240 MN/m
	C_{mx}		320 MN/m
	C_{my}		500 MN/m
	C_{mz}		656 MN/m
Ground	K		12 MN/m^3
Generator parameters and geometrical limits			
Δr	-23.6939		72.05 m < h_t < 150 m
A	58.7739		20.06° ≤ φ_u ≤ 20.06°
B	121.6289		35.08 m < r_o < 37.11 m

3. 2 Evaluation of parameters based on first natural frequency

Since the wind is the most significant excitation on the cooling tower shell, the natural frequency analysis needs to be evaluated by means of the finite element analysis program FEMAS 2000 [3]. The tower shell was discretized by 25 elements in the circumferential direction and 21 elements in the meridional direction.

Table 4. First natural frequencies of the selected models

h_t		108 m	113 m	118 m	123 m	128 m
f_1 [Hz]	15°	0.5868	0.5942	0.6078	0.6288	0.6528
	16°	0.6215	0.6217	0.6302	0.6468	0.6676
	17°	0.6499	0.6546	0.6571	0.6686	0.6848
	17.72°	0.6650	0.6792	0.6774	0.6848	0.6973
	18°	0.6719	0.6899	0.6865	0.6920	0.7030
	19°	0.6965	0.7261	0.7166	0.7162	-
	20°	0.7215	0.7520	0.7462	-	-

Table 4 shows the first natural frequencies of all 32 cooling towers selected. The first natural frequency tends to increase with increasing base lintel angle for each height of throat considered. The natural frequency increases as the throat height increases, when the angle of the base lintel is smaller than 18°. However the possible maximum height of throat will not necessarily yield the maximum first natural frequency. In the case that the angle is larger than 18°, the highest frequency was shown at the height of throat of 113 m. This parametric study definitely represents the relationship between the base lintel angle and the first natural frequency which indicates the insensitivity of the shell against wind excitation. However the influence of the throat height still cannot be generalized. In the view point of wind dynamics the prototype cooling tower shell geometry may be evaluated as reasonable.

For further understanding of the relationship between the dynamic characteristics and the shape of the tower, the generator equation (1) describing the radius over the height of the shell was investigated. Fig. 2 shows the radius r and the curvature r'' of the hyperbolic equation with varying height of throat for each selected angle of the base lintel. Obviously, the radius of the lower part of the shell decreases, when the angle of the base lintel increases. With increasing height of throat, the radius of the upper part of the shell decreases. This increase ratio of the upper part of the shell is much stronger than the decrease ratio in the lower shell. In the opposite case the radius of the lower part of shell decreases. Furthermore the curvature of the shell tends to be constant with increasing height of the throat and the base angle.

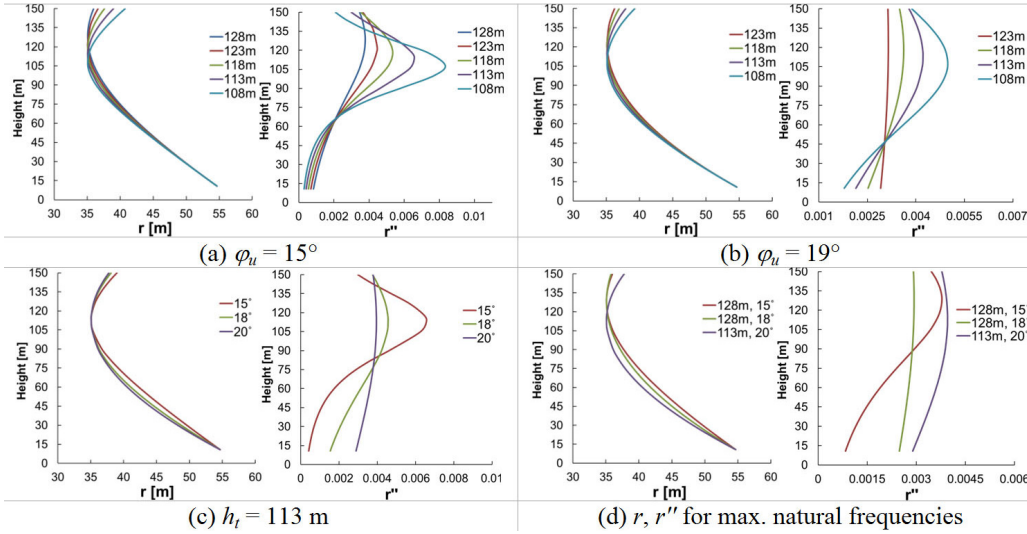

(a) $\varphi_u = 15°$ (b) $\varphi_u = 19°$

(c) $h_t = 113$ m (d) r, r'' for max. natural frequencies

Fig. 2. Comparison of generator characteristics

Because the radius of the shell directly determines the circumferential stiffness of the shell, the decreased radius in the upper part makes the shell effectively stiffer and consequently the frequencies will be increased. Such situation was indicated with increasing height of throat and increasing angle of base lintel. However, further increasing angle of base lintel, close to the limit, combined with a lower height of throat, will definitely enhance the horizontal shear stresses at the intersection from structure to soil. This would require more efforts for the foundation concept, like closed ring foundation or inclined piles. Such consequences are dependent on the local soil conditions and thus have not been considered in this study.

As a result, the geometric parameters for a hyperbolic generator with the small radius overall will yield a shell geometry with a higher first natural frequency and thus less wind-sensitivity. This can be achieved by describing the shell geometry with two hyperbolic equations. The radius of the lower shell can be minimized with a maximum angle of the base lintel and a minimum height of the throat, while the whole upper shell takes the minimum radius, almost like a cylinder shell.

4. Structural analysis of cooling towers with representative geometry

Due to the results of the previous investigations, three cooling towers with representative shell geometries were selected. Besides the prototype tower (Tower P) with h_t = 118 m, φ_u = 17.72° in Fig. 1, two towers with 'good' (Tower G) and 'bad' (Tower B) shell geometry with respect to natural frequency were chosen as shown in Fig. 3. Tower G is characterized by a

height at throat h_t = 113 m and an angle of the base lintel φ_u = 20.95°, while Tower B is described by h_t = 113 m and φ_u = 15°. The base lintel angles represent the maximum and minimum values at h_t = 113 m.

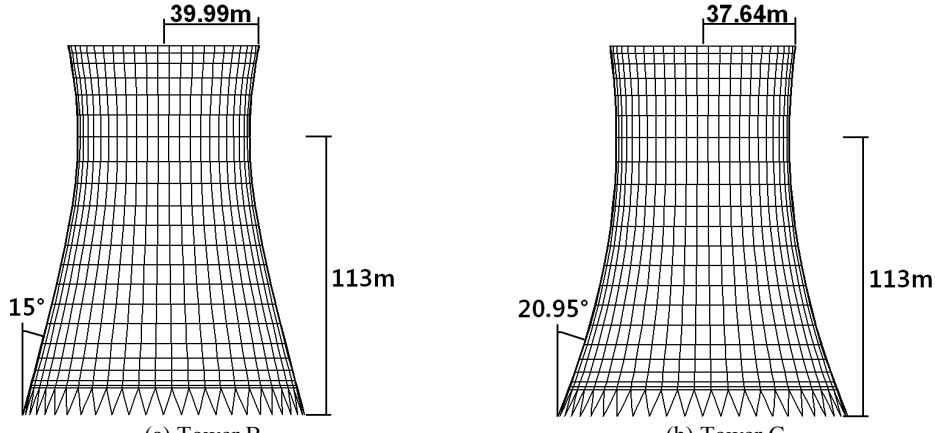

(a) Tower B (b) Tower G

Fig. 3. Generator parameters of Tower B and Tower G

4. 1 Linear analysis

According to VGB-BTR [5] the cooling tower is subjected to the dead weight G, quasi-static wind load W of wind zone I with the wind pressure distribution curve K1.1 and to temperature loads due to winter service conditions with a temperature difference of 45 K from the cooler outer to the warmer inner face.

Table 5 summarizes the results from the linear analysis of the selected towers. Besides the frequency analysis, the stability of the towers was evaluated by buckling analyses. When the angle of base lintel increases to the maximum angle of 20.95°, the natural frequency increases by 13.24 % compared to the prototype Tower P. At the angle of 15°, the natural frequency shows a 12.28 % reduction in the natural frequency. Buckling factors of all towers under the load combination of $G + W$ exceed 5, the requirements of the standard. With the maximum angle of base lintel of 20.95°, the stability capacity of Tower G increases by 4.78 % compared to the prototype Tower P. The amount of reinforcement required represents the stress distribution capacity and from the viewpoint of cost evaluation it is one of the most important criterions in the form-finding process.

Table 5. Limits of the structural parameters

	Tower B	Tower P	Tower G
First natural frequency f_1 [Hz]	0.5942	0.6774	0.7671
Buckling factor γ_b [-]	6.1157	6.9542	7.2868
Concrete volume V_c [m³]	8379	8295	8171
Reinforcement A_s [ton]	862.27	791.83	707.87

Fig. 4 shows the required amount of reinforcement, calculated under the consideration of the load combination $G + W + T$ and $G + 1.75W$ according to VGB-BTR [5], for the meridional and circumferential direction, as well as the total reinforcement over the height of the towers. Compared to the Tower P the amount of reinforcement required for Tower B increased by 8.90 %, while Tower G requires by 10.60 % less amount. Although all curve shapes for the total

amount look similar, the meridional and circumferential directions of Tower B totally differ from the others. This indicates also significant different stress distribution induced by the different geometry.

4. 2 Numerical finite element approach for damage analysis

Taking into account the true load process as well as a realistic material modelling for reinforced concrete the damage simulation will reproduce the load-bearing behaviour of the cooling tower more realistically. The complete tower has to be modelled as a reinforced concrete structure considering:

• a non-linear stress-strain relationship for concrete in compression,
• tension cracking after exceeding of concrete tensile strength,
• elasto-plastic stress-strain behaviour of the reinforcement,
• non-linear bond between reinforcement and concrete.

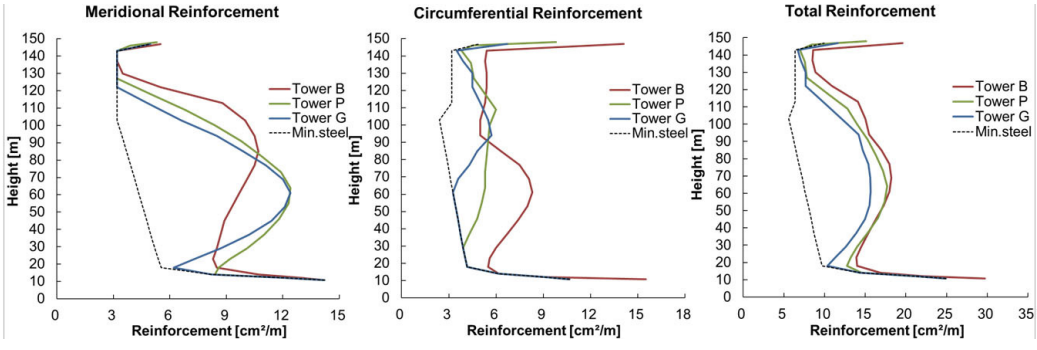

Fig. 4. Amount of reinforcement required

Each of these phenomena can be responsible for structural damages in the cooling tower followed by stress redistributions leaving the original (linear) design state. All these material processes are essentially irreversible, contributing to the crack-damage evolution in the shell. Thus the non-linear behaviour of concrete in compression should be coded in the applied computer program under consideration of elastic, plastic and micro-damage contributions. The reinforced steel model should cover elasto-plastic behaviour at least in a bi-linear mapping for cyclic processes, under special attention of the Bauschinger effect. To describe the nonlinearly fading bond, tension-stiffening concepts or improved non-linear bond laws should be applied. The used reinforced concrete model (Noh [6]) is briefly described as in the following.

• The concrete model used goes back to Darwin & Pecknold [7] and is a non-linear elasto-plastic damage model with material softening. The model is orthotropic in the principal stress directions for the biaxial state of stress. The behaviour of concrete in tension prior to cracking is assumed linear elastic. The principal tensile stress value governs the formation of tension cracking. Depending on the load and deformation history of the structure, the directions of cracks rotate according to the principal strain directions. Some cracks may close again due to local unloading or changing of the load direction.

• The reinforcement steel is idealized as smeared in the layered shell element. The Incremental uniaxial elasto-plastic constitutive law is applied taking kinematic hardening due to Prager as well as the Bauschinger effect into account.

• The bond effect is modelled indirectly as a participation of the concrete between the cracks (tension-stiffening) by modifying the steel model both for the monotonous and for the unidirectional cyclic loading. For the model set-up, the iterative computation concept with the

step-by-step integration of Eligehausen et al. [8] was employed, which allows the use of any complicated bond law.

This material non-linearity can be implemented by means of multi-layered model. The reinforced concrete in the tower shell is modelled as a layered continuum of uniaxial layers of reinforcement steel and of plane stress layers of concrete. The constitutive information in a material point has to be transformed to the finite element level and again upwards to the structure level. The applied homogenisation concept, which is efficiently realized by multi-level simulation technique, is described in Krätzig [9].

4. 3 Non-linear analysis

Fig. 8 shows the deformation curves under the increasing wind load, at the throat, z = 113 m on the windward side. As already recognized by the crack damage simulations of several cooling towers (Noh et al. [10]) the processes of crack formation in large cooling tower shells are in principal quite similar: The temperature load ΔT (45 K) under winter service condition leads to hair cracks on the whole outer face of the shell. The shells behave almost linearly up to the load level $\lambda \approx 1.30$. Afterwards wide cracks propagate horizontally on the windward side as well as vertically on the flanks, successively. They propagate and join together with increasing wind load.

In the analysis Tower G with the least amount of reinforcement is characterized by the best overall stiffness behavior. All three towers collapse approximately at the same wind load factor $\lambda \approx 2.90$, while the prototype tower and Tower G have approximately 26 % more ductility than Tower B.

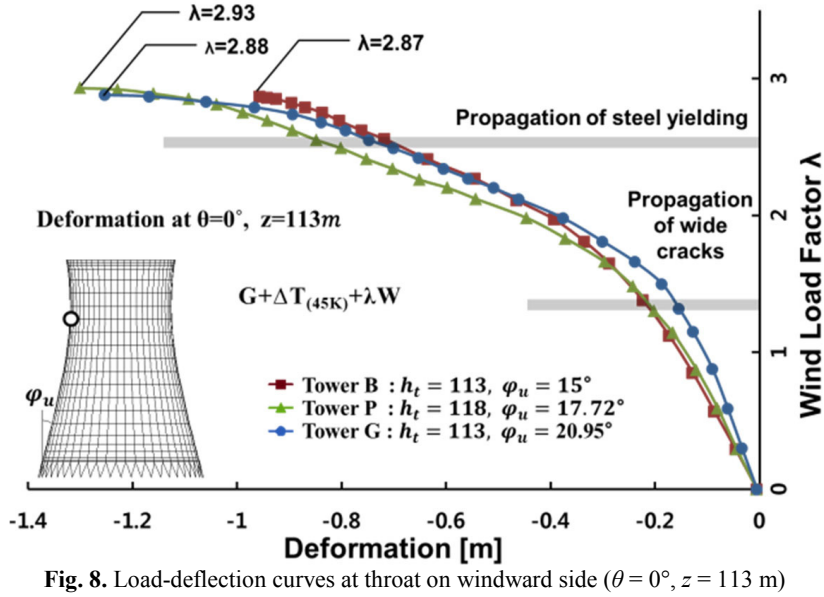

Fig. 8. Load-deflection curves at throat on windward side (θ = 0°, z = 113 m)

In Fig. 9 crack patterns on the outer face under wind load factor λ = 2.54 are pictured. For clarity, the cracks under winter service condition are represented only for the width greater than 0.1 mm. A comparison with the crack patterns shows the influence of geometry on the crack-damage process in the shell due to the stress redistribution. In Tower G with the maximum angle of base lintel, the cracks are distributed more widely than in Tower B, because the geometry of

Tower G allows that the stress may be easier transferred from the meridional direction to the circumferential direction and from the windward side to the flank region.

Cracking behavior is related to the cooling tower of deformation progress. In the deformation of all towers it can be observed that large deformation occurred at the upper shell and many wide cracks emerge at the top lintel in the lee region. In Tower P and G, as wind load increases, the region with large deformation moves from the upper part of the shell to the lower part. However in Tower B deformation is concentrated at the throat in the windward region. Thus Tower B with the most reinforcement collapses with a smaller displacement.

4. 4 Damage analysis

The damage process observed above may be quantitatively evaluated by the global damage indicator based on a set of the natural frequencies $\omega_i{}^d$, $1 \le i \le$ number of DOF in each damage state d. The damage indicator $D_{\omega i}$ defined in Noh et al. [10] was modified by the adoption of the modal contribution factor MCF_i, based on the external modal energy:

$$D_{\omega i}(V,\ d) = \frac{\omega_i^o - \omega_i^d}{\omega_i^o - \omega_i^f}, \tag{2}$$

$$D_{\omega,\ MCF} = \sum_{i=1}^{n} \left(D_{\omega i} \times MCF_i \right). \tag{3}$$

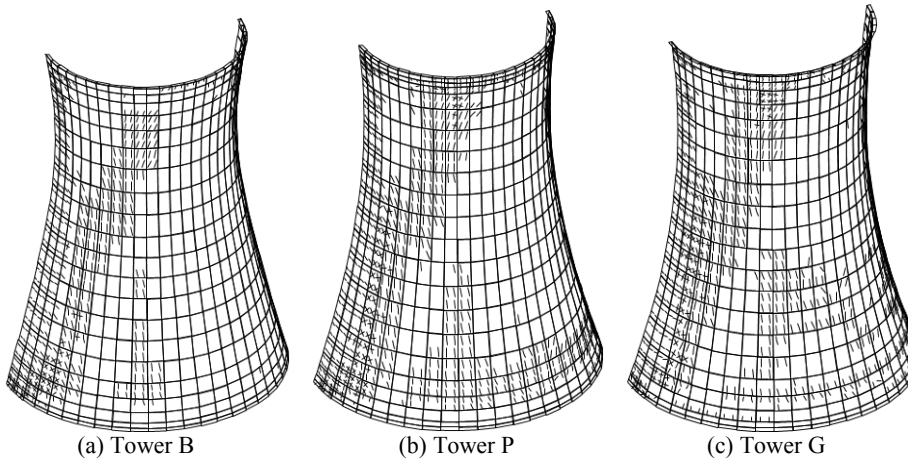

(a) Tower B (b) Tower P (c) Tower G

Fig. 9. Crack patterns (0.1 mm ≤ W_k) under λ = 2.54

In Eq. (2), $\omega_i{}^o$ and $\omega_i{}^f$ are the natural frequencies of the undamaged and collapse state, respectively, evaluated after the self-weight loading and just before the structural failure in the simulation. For the integration of all relevant damage responses expressed by the natural frequencies, we adopt the modal contribution factor MCF_i defined in Eq. (4). MCF_i expresses the ratio of the external modal energy induced by the i-th mode shape ϕ_i to the total external energy:

$$MCF_i = \frac{E_i}{\sum_{i=0}^{n} E_i} \quad \text{with} \quad E_i = V_i \cdot P_i. \tag{4}$$

Herein V_i and P_i indicate the contribution of the i-th mode shape ϕ_i to the total displacement V and the load intensity P, respectively. They can be obtained applying the procedure of the classical modal analysis in the structural dynamics, namely the modal expansion of the displacement and the excitation. In the time-independent nonlinear static analysis, V and V_i, however, depend upon the damage state d under the current load level P, instead of time t.

The contribution of the i-th mode shape to the displacement response V under the current load level P can be expressed using the modal coordinates q_i as Eq. (5). Combining these modal contributions gives the total displacement V:

$$V_i(d) = \varphi_i(d) \cdot q_i(d), \quad V(d) = \sum_{j=0}^{n} V_j(d) = \sum_{j=0}^{n} \varphi_i(d) \cdot q_i(d). \tag{5}$$

Under the consideration of the modal orthogonality of the mode shapes, the modal coordinates q_i associated with the i-th mode shape ϕ_i may be obtained using damage-invariant mass matrix M. Thus q_i and V_i can be obtained by using Eq. (6):

$$q_i = \frac{\varphi_i^T MV}{\varphi_i^T M \varphi_i}, \quad V_i = \frac{\varphi_i^T MV \varphi_i}{\varphi_i^T M \varphi_i}. \tag{6}$$

In a similar way, the static load P can be expanded using the modal coordinates q_i. Utilizing the orthogonal property of the modes, the contribution of the i-th mode shape to P may be expressed by P_i. Herein V_i and P_i as well as E_i are independent upon how the modes are normalized.

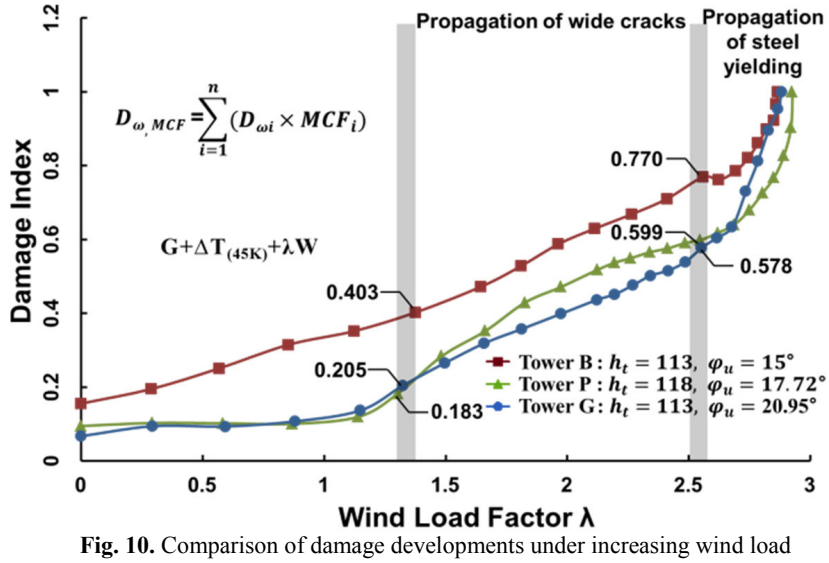

Fig. 10. Comparison of damage developments under increasing wind load

Fig. 10 shows the development of the global damage index $D_{\omega,MCF}$ based on the first 8 natural frequency under the load combination $G + \Delta T_{(45K)} + \lambda W$. The damage state of the tower is fairly influenced by the shell geometry even under the temperature load $G + \Delta T_{(45K)}$. This initial damage can be read from $D_{\omega,MCF}$ at $\lambda = 0.0$ in the figure: Tower B is damaged almost two times as Tower G with the least damage state, and increases linearly with increasing wind load. On the

other hand, damage states of Tower P and G remain without significant changes, up to wind load level of $\lambda \approx 1.20$. Thereafter they increase with the propagation of wide cracks. In this range the damage of Tower G is evidently smaller than for Tower P. From wind load level $\lambda \approx 2.54$ onwards, damage of three towers increase sharply, up to the collapse of the tower. From this global damage evaluation Tower B shows the highest damage state among three towers. This global damage behaviour results from the localization of the damage in Tower B, induced by insufficient capacity of the stress redistribution.

5. Conclusions

Hyperbolic generators with overall radii as small as possible – with respect to the thermo-dynamic requirements – will yield cooling tower shells with a higher first natural frequency and thus less wind-sensitivity. This can be achieved by describing the shell geometry with two hyperbolic equations, where the radius of the lower part of the shell is minimized with a maximum angle of the base lintel and a minimum height of the throat, while the upper part of the shell takes the minimum radius, almost like a cylinder shell. Linear and nonlinear analyses of three towers with the representative shell geometries verified as mentioned above: the tower with 'good' geometry needs less concrete and reinforcement masses than the others, but simultaneously shows a safer, more stable and more durable behavior both in linear and nonlinear analyses.

Acknowledgements

This research was supported by the Basic Science Research Program through the National Research Foundation of Korea (NRF) funded by the Ministry of Education, Science and Technology (2012-0008010).

References

[1] **D. Busch, R. Harte, W. B. Krätzig, U. Montag** New natural draft cooling tower of 200 m of height. Engineering Structures, Vol. 24, 2002, p. 1509-1522.

[2] **R. Harte., W. B. Krätzig** Large-scale cooling towers as part of an efficient and cleaner energy generating technology. Thin-Walled Structures, Vol. 40, 2002, p. 651-664.

[3] **H. Beem, C. Koenke, U. Montag, W. Zahlten** Femas 2000 - Finite Element Modules for General Structures. Institute for Statics and Dynamics, Ruhr – University Bochum, User – Handbook Release 3.0, 1996.

[4] **S. Y. Noh** Contribution to the Numerical Analysis of Damage Mechanisms of Natural Draught Cooling Towers. Ph. D. Thesis, RWTH Aachen, Febr. 2002, (in German).

[5] VGB 1997: Structural Design of Cooling Towers. BTR-Guideline VGB-R 610 Ue, VGB-PowerTech, Essen, 1997.

[6] **S. Y. Noh** Beitrag Zur Numerischen Analyse der Schadigungsmechanismen von Naturzugkuhltur-Men. Dr.-Ing. Thesis, RWTH Aachen, Germany, 2001.

[7] **D. Darwin, D. A. Pecknold** Inelastic Model for Cyclic Biaxial Loading of Reinforced Concrete. Civil Engineering Studies SRS Nr. 409, University of Illinois, 1974.

[8] **R. Eligehausen, E. P. Popov, V. V. Bertero** Local Bond Stress-Slip Relationships of Deformed Bars under Generalized Excitations. College of Engineering, University of California, 1983.

[9] **W. B. Krätzig** Multi-level modelling techniques for elasto-plastic structural responses. D. R. J. Owen, E. Onate, E. Hinton (editors). Computational Plasticity, Part 1, Int. Center for Num. Meth. Engng., Barcelona, Spain, 1997, p. 457-468.

[10] **S. Y. Noh, R. Harte, W. B. Krätzig, K. Meskouris** New design concept and damage assessment of large-scale cooling towers. Structural Engineering & Mechanics, Vol. 15, No. 1, 2003, p. 53-70.